Evidence for Subdomain Flexibility in *Drosophila melanogaster* Acetylcholinesterase

Jure Stojan,*,‡ Caroline Ladurantie,§ Omid Ranei Siadat,§,|| Laurent Paquereau,§ and Didier Fournier§

Institute of Biochemistry, Faculty of Medicine, University of Ljubljana, Vrazov trg 2, 1000 Ljubljana, Slovenia, and IPBS-CNRS, 205 Route de Narbonne, Toulouse, France

Received December 29, 2007; Revised Manuscript Received March 21, 2008

ABSTRACT: The catalytic domain of the acetylcholinesterases is composed of a single polypeptide chain, the folding of which determines two subdomains. We have linked these two subdomains by mutating two residues, I327 and D375, to cysteines, to form a disulfide bridge. As a consequence, the hydrodynamic radius of the protein was reduced, suggesting that there is some flexibility in the subdomain connection. In addition to the smaller size, the mutated protein is more stable than the wild-type protein. Therefore, the flexibility between the two domains is a weak point in terms of protein stability. As expected from the location of the disulfide bond at the rim of the active site, the kinetic studies show that it affects interactions with peripheral ligands and the entrance of some of the bulkier substrates, like *o*-nitrophenyl acetate. In addition, the mutations affect the catalytic step for *o*-nitrophenyl acetate and phosphorylation by organophosphates, suggesting that this movement between the two subdomains is connected with the cooperativity between the peripheral and catalytic sites.

The acetylcholinesterases (AChEs,[1] EC 3.1.1.7) are serine hydrolases that catalyze the hydrolysis of acetylcholine. These include some of the most efficient enzymes known (*1*). Structural studies have revealed that the AChE active site is buried in a 20-Å-deep gorge (*2*). At the entrance to the gorge, there is a nonproductive substrate binding site known as the peripheral anionic site (PAS), and at the bottom of the gorge, there is a productive site known as the acylation site. The main catalytic events are as follows: a substrate molecule first binds to the PAS (*3*) and then slides down to the acylation site, where it is cleaved, with the products escaping from the protein via the gorge. The gorge is too narrow to allow the crossing of a substrate molecule en route to the bottom and a product molecule en route to the exit. Consequently, their trafficking between the two sites leads to complex kinetics that provides informative data relating to substrate hydrolysis across a wide range of concentrations, as at very high concentrations this results in a traffic-jam effect that leads to inhibition (*4, 5*).

Despite the AChEs being some of the most studied enzymes, the significance of conformational changes in relation to substrate hydrolysis remains puzzling. Rearrangements within the protein have mainly been used to explain the exit of the products. An opening in the so-called omega loop [residues 67−94 in *Torpedo californica* AChE (*Tc*AChE)] to produce a "back door" was proposed on the basis of molecular dynamics simulations (*6*). Likewise, a route for exit of the second product, acetate, was proposed just behind the "acyl pocket" (*7*), involving the loop of residues 279−291, which is disordered and thus flexible in the structure of *Tc*AChE complexed with a galanthamine derivative (*8*). Moreover, the residual catalytic activity seen for a complex of AChE with the gorge-capping mamba venom toxin, fasciculin (*9*−*13*), can maybe be explained by molecular breathing. Later molecular dynamics studies have provided further evidence of loop movements creating doors for product exit (*14*−*17*). In contrast, much evidence has suggested that conformational changes are not involved during substrate hydrolysis. Kinetic models can describe the data without assuming classical conformational motions (*4, 18*). Resolved crystal structures in the absence and presence of ligands do not reveal backbone variations: a low AChE activity has been recorded within the crystal, where most of the backbone motions are prevented by the tight molecular packing (*19*) and despite a substantially decreased level of diffusion, due to reduced water content. Omega loop fixation by the introduction of an additional disulfide bond (G80C/V431C in *Torpedo marmorata* AChE) did not impair substrate hydrolysis (*20*−*22*). Therefore, the conformational movements beyond changing side chain positions remain controversial.

We recently engineered another disulfide bond between I327 and D375 (I287 and G335, respectively, *Tc*AChE numbering) in *Drosophila* AChE, to improve the use of the enzyme in biosensors for detection of insecticide residues. This disulfide bond provides greater stability, measured as resistance to high temperature, to organic solvent, to urea, and to protease digestion (*23*). The C327−C375 disulfide bond is located at the rim of the active site gorge, where it links two subdomains that participate in the walls of the

* To whom correspondence should be addressed. Telephone: +386 1 5437649. Fax: +386 1 5437641. E-mail: stojan@mf.uni-lj.si.
‡ University of Ljubljana.
§ IPBS-CNRS.
|| Current address: Department of Biology, Faculty of Basic Sciences, Shahed University, Tehran, Iran.

[1] Abbreviations: AChE, acetylcholinesterase; cc-mutant, I327C/D375C DmAChE; ATCh, acetylthiocholine; BSA, bovine serum albumin; PAS, peripheral anionic site; SDS, sodium dodecyl sulfate.

10.1021/bi7025479 CCC: $40.75
Published on Web 04/26/2008

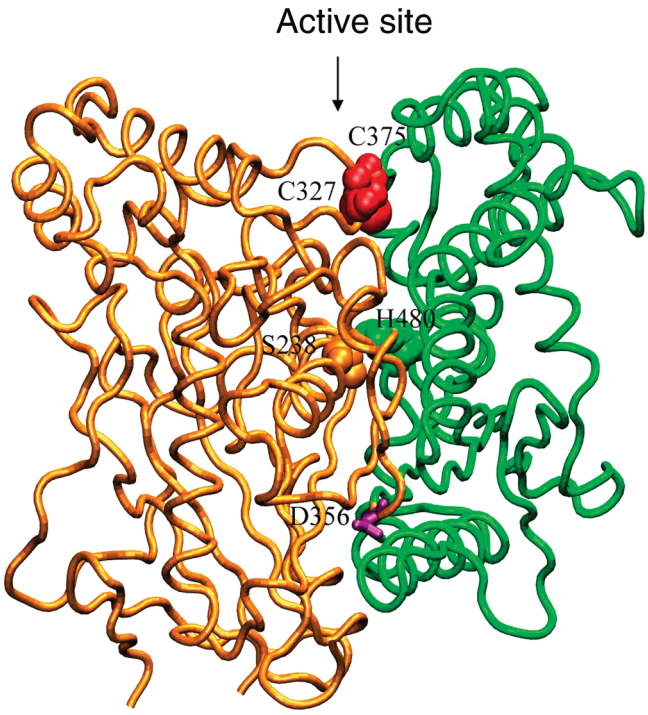

FIGURE 1: Position of the new disulfide bridge (I327C−D375C). The backbones of the two subdomains are presented in two different colors, considering D356 as the border. Atoms of the two cysteines are depicted as red spheres. Amino acids of the catalytic site (serine 238 and histidine 480) are highlighted.

active site (Figure 1). Here we analyze the consequences of this link for protein structure and activity.

EXPERIMENTAL PROCEDURES

Protein Production and Purification. Engineering a disulfide bond at positions 327 and 375 was pursued because the distance between the two Cβ atoms is 3.77 Å and the two amino acids are not conserved in the cholinesterase family. Mutations of I327 and D375 to cysteines were introduced by site-directed mutagenesis using the QuickChange XL kit by following its instruction (Stratagene). The formation of the disulfide bond was confirmed by titration with Ellman's reagent in the presence of 6 M urea (*23*). The cDNAs encoding *Dm*AChE and its cc-mutant were expressed with the baculovirus system (*24*). For both of these proteins, we expressed a soluble dimeric form deprived of a hydrophobic peptide at the C-terminal and with a three-histidine tag replacing the loop from amino acid 103 to 136 using single-strand mutagenesis (*25*). This external loop is at the opposite side of the molecule with respect to the active site entrance, and its deletion affects neither the activity nor the stability of the enzyme. The same was true with the truncated C-terminal peptide. Secreted AChEs were purified to homogeneity using the following steps: ammonium sulfate precipitation, ultrafiltration with a 10 kDa cutoff membrane, affinity chromatography with procainamide as a ligand, NTA-nickel chromatography, and anion exchange chromatography (*26*). Residue numbering followed that of the mature protein, with *T. californica* AChE numbering as a reference.

Enzyme Activity. The concentrations of the enzymes were determined by active site titration using high-affinity irreversible inhibitors (*27*). The progress of substrate hydrolysis was followed at 25 °C in 25 mM sodium phosphate buffer (pH 7) containing 1 mg/mL bovine serum albumin (BSA). Hydrolysis of acetylthiocholine (ATCh), an analogue of the neurotransmitter that allows easy detection of the reaction product, was studied spectrophotometrically at 412 nm using the method of Ellman et al. (*28*), at substrate concentrations ranging from 2 μM to 300 mM, in 1 cm path length cuvettes. The activity was measured for 1 min after addition of the enzyme to the reaction mixture. The experiments in the presence of different reversible inhibitors were performed under the same conditions as the control experiments without them. Scheme 1 and the corresponding equation (see the expression for *A* in the Appendix, and ref *29*) were used to describe the dependence of initial enzyme activity at different substrate concentrations (pS curves) in the absence and presence of inhibitors. Hydrolysis of *o*-nitrophenyl acetate in 25 mM phosphate buffer (pH 7) and 5% DMSO was monitored by the formation of *o*-nitrophenolate at 405 nm, with the Michaelis−Menten equation used for the analysis.

The inhibition of *Dm*AChE by carbamates and organophosphates can be considered irreversible during the first 15 min. The disappearance of free enzyme follows second-order kinetics. The rate of inhibition was estimated by incubating the enzyme with various insecticide inhibitors (see Table 1) at 25 °C in 25 mM phosphate buffer (pH 7). The variations in the activity of the remaining free enzyme over time were estimated by sampling aliquots at various times and recording the remaining activities with 1 mM ATCh, since the remaining activity was proportional to the remaining free enzyme concentration. Kinetic studies were performed with at least three concentrations of inhibitor. The values of k_i were estimated by multiple nonlinear regression analysis, where the initial inhibitor concentration and time were independent variables. Data were collected until the standard deviation of the k_i value became less than 10%.

To determine whether the mutation predominantly affected the affinity of the insecticide or formation of a covalent bond with the catalytic serine, we compared the initial rates obtained from the activity measurements of ATCh hydrolysis in the presence of paraoxon by both the wild type and the mutated enzyme. For the analysis, we used our two-binding-site model, allowing ATCh and paraoxon to interact with either site, both with the free and with the acetylated enzyme (Scheme 1). Additionally, we measured the time course of product formation in the presence of paraoxon until these curves became parallel to the *x* axis, but virtually within the linearity of curves without paraoxon. In the progress curve analysis, we used the same reaction scheme that was enlarged by the steps for irreversible enzyme inhibition when paraoxon was bound to the active site (see the scheme in the Appendix). The analysis itself was carried out by fitting the time course for product formation, obtained by numerical integration of model specific differential equations, to the experimental progress curves and checked by using the derived explicit progress curve equation (see the Appendix). To find the solution that would adequately reproduce all our kinetic data, we kept in the progress curve analysis the parameters as determined from the initial rate data. Thus, only k_i and $e = f$ are left to be evaluated.

Estimation of the Hydrodynamic Sizes of Proteins. Four types of analyses were performed to estimate the relative sizes of the wild type and cc-mutant of *Dm*AChE. (i) Electrophoresis of native AChEs using 4 to 25% polyacry-

Scheme 1: Substrate Hydrolysis by Cholinesterases in the Presence of a Reversible Inhibitor that Competes at the Peripheral Anionic and the Catalytic Site of the Free and Acetylated Enzyme[a]

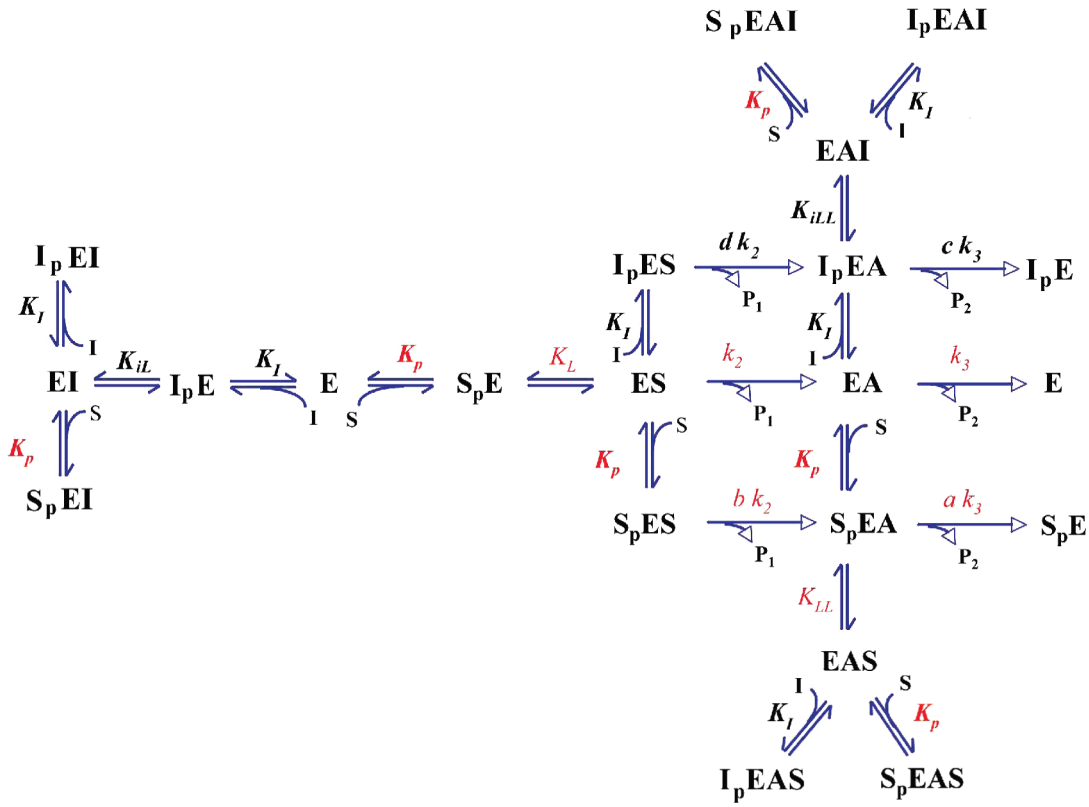

[a] Abbreviations: E, free enzyme and its complexes; S, substrate; I, inhibitor; SpE and IpE, substrate and inhibitor bound to the peripheral anionic site, respectively; ES and EI, substrate and inhibitor bound to the catalytic site, respectively; EA, acetylated enzyme and its complexes.

Table 1: Effects of the cc-Mutation on the Second-Order Rate Constants for the Carbamoylation and Phosphorylation of the Active Site Serine by Various Pesticide Inhibitors

	k_i (μM^{-1} min^{-1})		
	wild type	cc-mutant	ratio
Carbamates			
carbaryl	0.055	0.058	1.05
propoxur	0.58	0.5	0.86
aldicarbe	0.02	0.031	1.55
pirimicarbe	0.19	0.052	0.27
Organophosphates			
dichlorvos	2.25	19.74	8.77
terbufos oxon	0.008	0.024	3.00
methamidophos	0.0008	0.004	5.00
monocrotophos	0.007	0.025	3.57
omethoate	0.016	0.07	4.38
paraoxon	0.97	13.52	13.94
malaoxon	1.02	4.1	4.02
profenofos	0.074	0.59	7.97
coumaphos	3.8	37	9.74
azinphos methyl oxon	26	74	2.85

lamide gradient gels was performed, according to the technique of Hames (*30*), at 200 V for 16 h in Tris-borate buffer (pH 8) containing 0.1% deoxycholate, as a nondenaturing detergent. The active *Dm*AChE forms were detected by their enzymatic activities using the method of Karnovsky and Roots (*31*), and the molecular weight protein standards were stained using Coomassie Brilliant Blue. (ii) Sodium dodecyl sulfate (SDS) gel electrophoresis was performed on 10% acrylamide gels, and the migration was followed at 50 V and room temperature. (iii) Gel filtration was performed with Sephacryl S-300 and S-200 in 25 mM phosphate buffer (pH 7). (iv) Dynamic light scattering was carried out using a nanosizer dynapro MS/X apparatus from Protein Solutions Inc. The measurements were taken at a wavelength of 825.7 nm with a detection angle of 90°. Proteins were presented as a particle mass.

RESULTS

Effects of the C327−C375 Disulfide Bridge on the Size of the Protein. We first hypothesized that the increased stability of the mutant could be due to the formation of a higher degree of polymerization. This could involve the formation of a tetramer, since new cysteines are located at the protein surface. To test this, we estimated the size and hydrodynamic volume of the mutant. Gel filtration, SDS gel electrophoresis without a reducing agent, and nondenaturing electrophoresis showed that the cysteines introduced did not form new intersubunit interactions in the mutants. However, as we did not find slowly migrating species, we would be surprised to find the reverse. Namely, by native electrophoresis, the cc-mutant migrated faster than the wild type. This could not be explained by a charge modification due to the mutation of an aspartic acid to a cysteine, since the mutant should migrate slower toward the anode. Therefore, it was possible that the mutation reduced the size of the protein. This hypothesis was tested using different methods for comparing the hydrodynamic volumes of the cc-mutant and the wild type. In native gradient gel electrophoresis, the proteins migrate until they remain stuck by the gel mesh. The wild-type

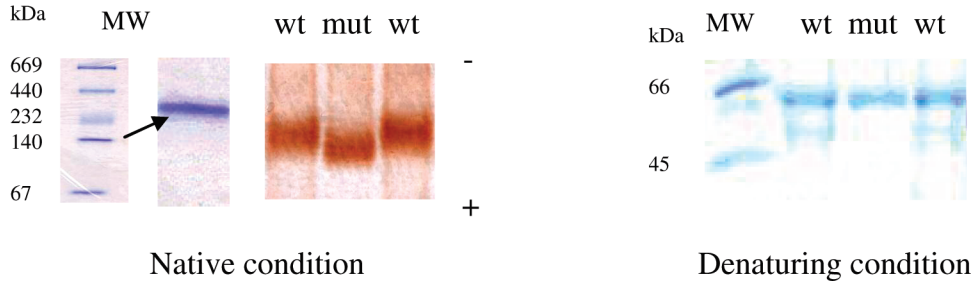

FIGURE 2: Effects of the new disulfide bridge (I327C−D375C) on the hydrodynamic volume of the protein assessed by native gel gradient electrophoresis. The middle lane of each picture shows the position of the mutant, and the other two lanes contained wild-type AChE. The gel is stained for AChE activity under native conditions, and the molecular mass markers are stained with Coomassie Brilliant Blue. A SDS−PAGE gel is presented as a reference for the migration under denaturing conditions.

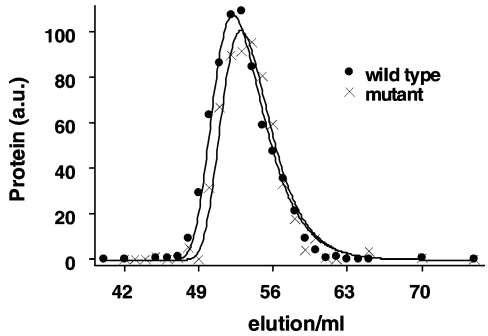

FIGURE 3: Size exclusion chromatography using Sepharose S300 gel. The mutant is delayed compared to the wild type and should thus be smaller.

protein migrates as a 140 kDa protein, corresponding to the dimeric form of *Dm*AChE (*32*). In repeating this analysis with six batches of the enzyme from different productions and purifications, we found the cc-mutant always ran faster than the wild type, suggesting that the addition of the disulfide bond did indeed compact the protein (Figure 2). To verify that this smaller size originates from the tertiary structure of the protein, rather than from the length of the polypeptide, SDS−PAGE was performed under denaturing conditions. As one can see in Figure 2, the migration rates of these two proteins do not differ. This also excludes the possibility of an undesired charge-altering mutation during the mutagenesis.

Changes in electrophoretic mobility under native conditions can originate from factors other than the size of a protein. These could arise from the charge affinity with the gel or with other components present in the system. Although these factors were theoretically eliminated by long-term electrophoresis in a gradient gel (more than 16 h), we could not eliminate their participation in the differential migration of the mutants.

We then performed size-exclusion chromatography. Five analyses were performed independently, i.e., with different protein batches, obtained from two mutagenesis experiments, using either Sephacryl S300 or S200 gel. In each comparative experiment, the mutant appeared to be smaller than the wild-type protein (Figure 3). Finally, dynamic light scattering, a technique used to assess the volume of a protein, was used. The hydrodynamic radius of the mutant was 4.15 ± 0.5 nm, with that of the wild type being 5.03 ± 0.7 nm, again the mutant always smaller that the wild type.

Enzyme Activity Effects. Surprisingly, the mutations introduced did not significantly affect the hydrolysis of the substrate ATCh. The rate of hydrolysis by 1 nM enzyme at 1 mM ATCh in 25 mM phosphate buffer (pH 7) at 25 °C was estimated to be 1060 ± 215 s^{-1} using several organophosphates as titrating agents (triazophos oxon, coumaphos oxon, and azinphos methyl oxon). A very similar rate was obtained under the same conditions for the wild type (976 ± 206 s^{-1}).

To determine whether the disulfide bridge affects the trafficking of the substrate and product molecules in the active site gorge, we analyzed the pS curves according to a previously suggested model that takes into account (i) the presence of two substrate binding sites, (ii) the hindrance of choline exit when the peripheral site was occupied by a substrate molecule, (iii) the acceleration of deacylation by a substrate molecule bound at the peripheral site, and (iv) the block of deacetylation when a second substrate molecule was attached to Trp83 (Trp84 for the *Torpedo* enzyme) at the catalytic anionic site, or when the active site was fully occupied (Scheme 1) (*33*).

Kinetics analyses were performed in the presence of various substrates (ATCh, butyrylthiocholine, and *o*-nitrophenylacetate), products (choline), and inhibitors specific for the peripheral site (propidium, aflatoxin, and Triton X-100) or specific for the catalytic site (edrophonium).

The cc-mutation had practically no effect on the hydrolysis of substrate ATCh or butyrylthiothiocholine (Figure 4 and Table 2). However, for the hydrolysis of *o*-nitrophenylacetate, the apparent K_m was decreased (20%) and the k_{cat} was increased (30%), thus making the cc-mutant more efficient (Figure 4). When the inhibitors were tested, there was no effect of the cc-mutation on product inhibition or of the active site-directed reversible inhibitor edrophonium. In contrast, the cysteine bridge introduced at the rim of the active site gorge affected the binding of ligands specific for the peripheral anionic site. The K_i of propidium increased from 5.7 nM to 0.4 μM, while the equivalent parameter for Triton X-100 decreased from 0.4 to 0.07%; the K_i for aflatoxin increased from 6 to 14 μM (Figure 4).

In chemical terms, the carbamates and organophosphorus compounds use the same reaction pathways as acetylcholine does. The catalytic serine located at the bottom of the active site is carbamoylated or phosphorylated, in the same way it is acetylated by acetylcholine. As decarbamoylation and dephosphorylation take a long time, measuring the remaining activity upon exposure with these compounds permits an estimation of their rates of serine acylation. The rate constant for carbamoylation by four selected agents did not significantly change with the cc-mutation. However, it is clear from Table 1 that the second-order overall phosphorylation rate

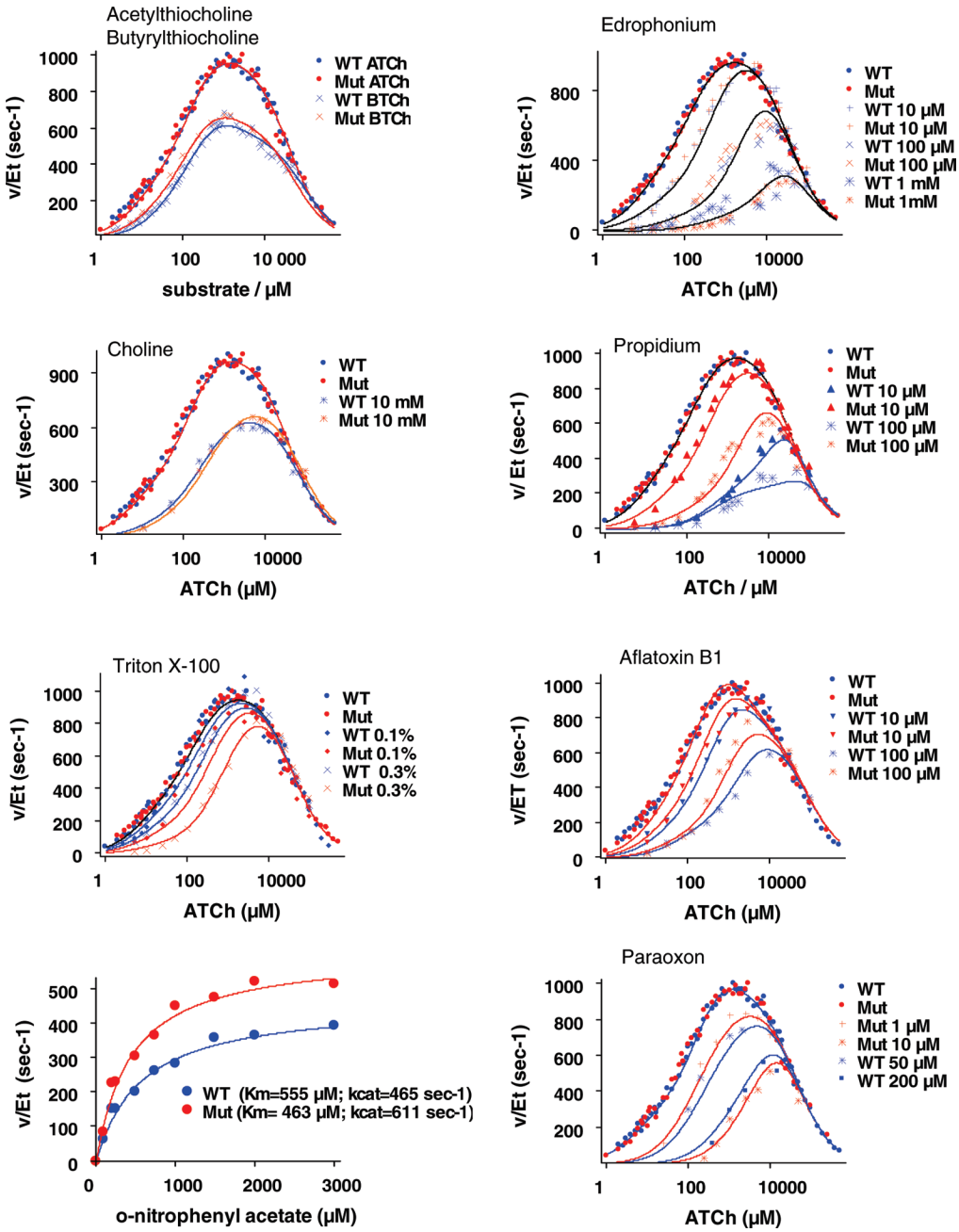

FIGURE 4: Dependence of the initial enzyme activity at different substrate concentrations (pS curves) for the wild type and the I327C/D375C mutant in the presence of the substrates acetylthiocholine and butyrylthiocholine, the product choline, and edrophonium, an inhibitor specific for the catalytic site, and some inhibitors specific for the peripheral anionic site (propidium, TX-100, and aflatoxin). The fitting of the v/Et vs. [S] curves in the presence of *o*-nitrophenyl acetate was performed according to the Michaelis−Menten equation.

constant is substantially increased for all of the organophosphates that were tested, and especially for paraoxon.

To determine whether the affinity or formation of the covalent bond is changed by the mutation, we compared the initial rates of ATCh hydrolysis by the two enzymes in the presence of paraoxon (Figure 4). It turned out that the affinity of paraoxon toward PAS is better for the cc-mutant (K_{ip} = 0.8 μM) than for the wild type (K_{ip} = 35.1 μM). On the other hand, the partition coefficient for the reversible paraoxon binding between the peripheral and the catalytic sites is some 6 times in favor of the wild type (K_{iL} for the cc-mutant, 1.84; K_{iL} for the wild type, 0.31), although the affinity of paraoxon for the catalytic site (K_iK_{iL}) remained better in the cc-mutant (1.5 μM vs 11 μM). In addition to the affinity ratio at the active site (7.5), the first-order phosphorylation rate constant was also 3.5 times faster in the cc-mutant. All these constants are included in the values of the bimolecular phosphorylation constants, and those which were calculated from the progress curve analysis (k_i, K_i, and K_{iL}) agree well with the values from dilution experiments (see Table 2). Consequently, the increased sensitivity of our cc-mutant was predominantly due to increased affinity and also to a rather small increase in the phosphorylation rate. It should be stressed that we have confirmed these findings by progress curve analysis using a numerical integration method and checked by fitting the explicit equation (see the Appendix and Supporting Information) to the set of time-dependent product formation curves of wild-type and cc-mutant *Dm*AChE in the presence of paraoxon.

Table 2: Characteristic Kinetic Constants for the Hydrolysis of ATCh by the Wild Type and the cc-Mutant of *Dm*AChE in the Absence and Presence of Peripheral Site Inhibitor Propidium and Active Site Inhibitor Paraoxon[a]

	wild type	cc-mutant
Acetylthiocholine (initial rates)		
k_3 (s^{-1})	413.7 ± 36.2	507.4 ± 35.7
K_p (mM)	0.182 ± 0.023	0.229 ± 0.033
K_L	5.21 ± 2.02	4.91 ± 1.38
K_{LL}	171.6 ± 23.7	170.5 ± 27.5
k_2 (s^{-1})	61550 ± 18782	51188 ± 11082
a	3.19 ± 0.26	2.75 ± 0.23
b	0.045 ± 0.012	0.028 ± 0.009
$k_{cat}/K_m = k_2/K_p/K_L$ (M^{-1} s^{-1})	6.48×10^7	4.46×10^7
Propidium (initial rates)		
K_i (nM)	5.7 ± 0.3	443 ± 39
c	3.67 ± 0.11	1.22 ± 0.19
d	0.013 ± 0.001	0.0037 ± 0.0006
Paraoxon (initial rates)		
K_i (μM)	35.1 ± 11.7	0.804 ± 0.275
K_{iL}	0.313 ± 0.0147	1.84 ± 0.95
K_{iLL}	not present	not present
c	a	a
d	b	b
$K_s = K_iK_{iL}$ (μM)	11.0	0.15
Paraoxon (progress curves)		
k_i (s^{-1})	0.16 ± 0.003	0.54 ± 0.01
$e = f$	0.056 ± 0.001	0.156 ± 0.0004
$k_i/K_i/K_{iL}$ (μM^{-1} min^{-1})	0.86	22.0
Paraoxon (dilution experiments)		
$k_{phosphorylation}$ (μM^{-1} min^{-1})	0.97	13.52

[a] The constants were determined in a multistep analysis in the order listed in the table. The previously determined constants were then fixed in the subsequent steps. The overall second-order phosphorylation rate constant is given for the comparison with the value obtained from the initial rate data combined with progress curve data.

DISCUSSION

Mechanism of Stabilization by the Disulfide Bond. Disulfide bonds are common to many extracellular proteins, where they stabilize the folded protein conformation according to several mechanisms. They serve to stabilize the native conformation by lowering the entropy of the unfolded form (*34*). This mechanism should not apply to cholinesterases, since their denaturation is irreversible. Disulfide bonds also stabilize proteins, because they increase their packing load, with a reduction in the volume and number of cavities that are energetically unfavorable due to a loss of van der Walls contacts. Thus, proteins from thermophilic species have fewer and smaller cavities than their mesophilic counterparts (*35*−*39*). Although this mechanism cannot be totally excluded, it is quite improbable for cholinesterases, since the active site is a large open cavity in the core of a protein filled with water molecules. The mechanism for a decreased rate of unfolding (*40, 41*), however, appears appropriate because cholinesterases denature irreversibly. An additional disulfide bond would decrease the entropy of the folded forms and would then reduce the probability of unfolding though the molten globule intermediate.

AChE Should Be in Its Compact Form in the Crystal. The distance between the two Cβ atoms of I327 and D375 in the resolved crystal structure of native *Dm*AChE (PDB entry 1QO9) is 3.77 Å. This is a suitable distance for the formation of a disulfide bridge upon mutation of both residues into cysteines. In silico mutation and dynamics showed no change in the backbone structure, suggesting that the disulfide bond did not influence the conformation of the protein in the crystal. In solution, the disulfide bond makes the protein more compact because the hydrodynamic radius decreases from 5.0 to 4.2 nm. It appears that the conformation of the mutant with the newly introduced disulfide bridge in a buffer solution resembles the crystal conformation of the wild type. This is consistent with the very similar kinetics of ATCh hydrolysis in solution and with the observation of the activity and substrate trafficking following crystal soaking in a solution with the substrate or with analogues (*5*).

The Disulfide Bond Affects the Binding of Ligands Specific for the Peripheral Site. Ligand binding to the peripheral site is modified by the presence of the disulfide bond. For example, the affinities for propidium and aflatoxin decreased, the affinities for TX-100 and paraoxon increased, and the affinity of ATCh for the peripheral site remained unchanged. One can hypothesize that this is a direct effect, because of the differences in size, mobility, and charge between the side chains of Cys and Ile or Asp residues, but one can also consider the effect to be indirect, because the newly established disulfide bridge could change the architecture of the entrance into the active site. Sometimes, peripheral site ligands are difficult to "see" in crystal structures, even if the packing problem is overcome. A selective change in the affinity of the compacted form for the distinct ligands might be an explanation.

Allostery between the Peripheral Site and the Catalytic Site. It has been shown that binding of some ligands at the peripheral site can increase the rate of phosphorylation (*42, 43*) and sulfonylation (*44*) and that some mutations at the peripheral site may do the same (*45*). Kinetic data obtained with different cholinesterases have also been interpreted as an increase in the level of serine deacetylation upon binding of the substrate to the PAS. Strong evidence has come from studies of decarbamoylation in the presence of a substrate analogue (*46*), and from analysis of simultaneous effects on substrate hydrolysis by various inhibitors (*46*). All of these suggest a sort of cooperativity between the peripheral and catalytic sites. The analysis of the cc-mutant data produced a new indication for this phenomenon, since we saw an increase in the extent of catalysis of *o*-nitrophenyl acetate and an increase in the phosphorylation rate. Our interpretation may provide a structural model for allostery in the cholinesterases, but it might also be considered more widely. We suggest that there is complementary breathing between the two *Dm*AChE domains, bordered by Asn356. Some key residues for the catalysis, such as the active site serine, are situated in the N-terminal domain, while others, such as the histidine of the catalytic triad, are in the C-terminal domain (Figure 1). Thus, the breathing affects the relative positions of these essential residues and consequently the catalytic efficiency. Binding of a ligand to the peripheral site may stabilize a conformation different from that of the free enzyme.

The Disulfide Bridge Increases the Sensitivity to Organophosphate Compounds. We have shown previously that the introduction of the C327−C375 disulfide bond in *Dm*AChE does not affect protein production but does increase protein stability (*23*). Here, we show that this mutation also increases sensitivity to organophosphates

Scheme A1: Substrate Hydrolysis by the Cholinesterases in the Presence of an Irreversible Inhibitor that Competes at the Catalytic Site and the Peripheral Anionic Site of the Free and Acetylated Enzyme[a]

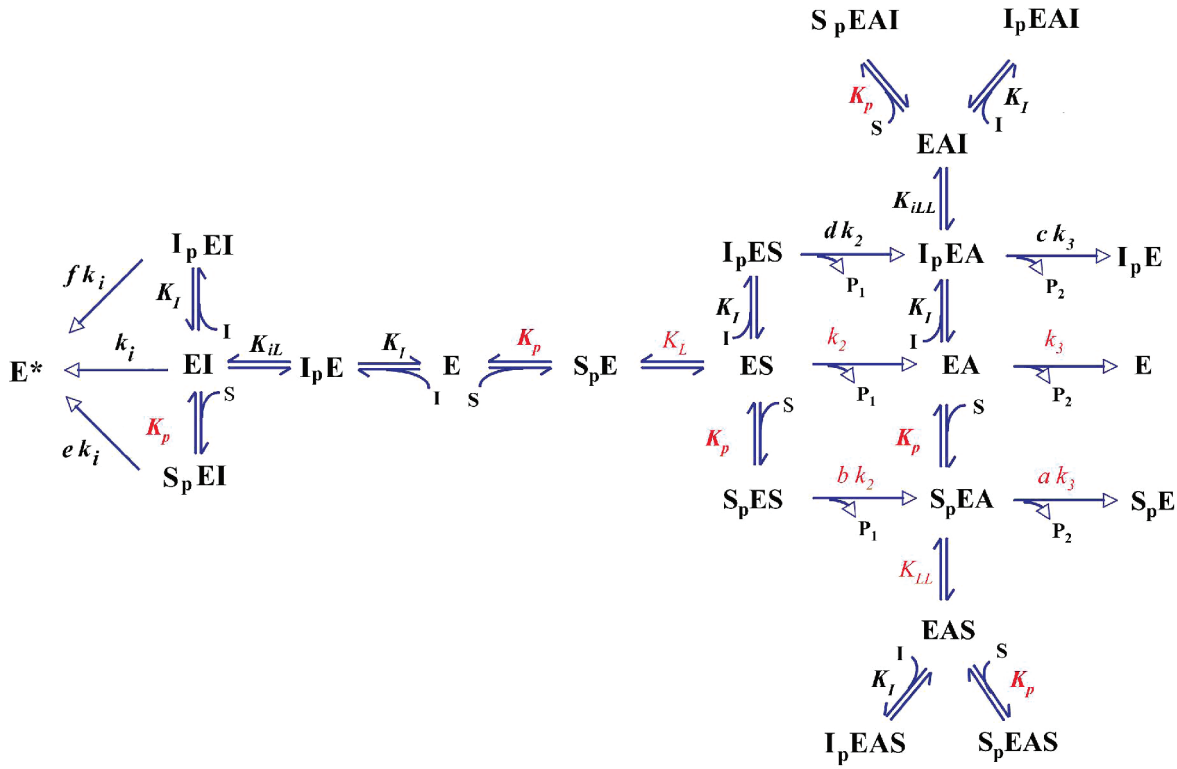

[a] Abbreviations: E, free enzyme and its complexes; S, substrate; I, inhibitor; SpE and IpE, substrate and inhibitor bound to the peripheral anionic site, respectively; ES and EI, substrate and inhibitor bound to the catalytic site, respectively; EA, acetylated enzyme and its complexes; E*, irreversibly inhibited enzyme.

without significantly affecting ATCh hydrolysis and carbamoylation. It appears consistent that only phosphorylation is enhanced in a more compact enzyme. Considering the breathing of the enzyme molecule, it appears that organophosphorous compounds that form a pentahedral adduct induce less relaxation in the mutant than in the wild type. This, in turn, preserves energy to conduct the organophosphate toward the transition state.

Finally, it should be noted that organophosphate pesticides are widely used in crop protection, to control various pests, such as insects, acarids, and nematodes. They can be detected with biosensors using AChE as the biological element (*47*). The enzyme should be easy to produce and should be stable and sensitive. All of these characteristics are improved by introduction of a new disulfide bridge, so the I327C/D375C mutant of DmAChE is especially interesting for use in biosensors.

APPENDIX

K_P and K_I are the dissociation constants for the binding of substrate and inhibitor to the peripheral anionic site, respectively. K_L, K_{LL}, K_{iL}, and K_{iLL} are the partition coefficients for the reversible binding between the peripheral anionic site and the catalytic site. k_2, k_3, and k_i are the rate constants, and a–f are the proportional factors.

The derived explicit equation for the time course of product formation, neglecting the depletion of substrate and inhibitor, is as follows:

$$[P]_t = \frac{A}{B}(1 - e^{-Bt})$$

In this equation

$$A = \frac{k_{cat}[E]_0[S]}{[S] + K_m}$$

$$B = \frac{k_i\frac{[I]}{K_{iL}K_I}\left(1 + e\frac{[S]}{K_P} + f\frac{[I]}{K_{IP}}\right)}{k_2[S]\left(1 + b\frac{[S]}{K_P} + d\frac{[I]}{K_I}\right)}G + H$$

$$k_3K_PK_L\left(1 + a\frac{[S]}{K_P} + c\frac{[I]}{K_I}\right)$$

where

$$k_{cat} = \frac{k_2k_3}{k_2M + k_3N}$$

$$K_m = \frac{\dfrac{k_3K_PK_L\left(1 + \dfrac{(I)}{K_I} + \dfrac{(I)}{K_IK_{iL}} + \dfrac{(I)^2}{K_I^2K_{iL}}\right)}{1 + b\dfrac{[S]}{K_p} + d\dfrac{[I]}{K_I}}}{k_2M + k_3N}$$

and

$$G = 1 + \frac{[S]}{K_P} + \frac{[S]}{K_PK_L} + \frac{[S]^2}{K_P^2K_L} + \frac{[S][I]}{K_PK_LK_I} + \frac{[I]}{K_I} + \frac{[I]}{K_IK_{iL}} + \frac{[I]^2}{K_I^2K_{iL}} + \frac{[S][I]}{K_PK_IK_{iL}}$$

$$H = 1 + \frac{[S]}{K_P} + \frac{[S]}{K_P K_{LL}} + \frac{[S]^2}{K_P^2 K_{LL}} + \frac{[S][I]}{K_P K_{LL} K_I} + \frac{[I]}{K_I} + \frac{[I]}{K_I K_{iLL}} + \frac{[I]^2}{K_I^2 K_{iLL}} + \frac{[S][I]}{K_P K_I K_{iLL}}$$

$$M = \frac{H}{1 + a\frac{[S]}{K_P} + c\frac{[I]}{K_I}}$$

$$N = \frac{1 + K_L + \frac{[S]}{K_P} + \frac{[I]}{K_I} + K_L\frac{[I]}{K_I K_{iL}}}{1 + b\frac{[S]}{K_P} + d\frac{[I]}{K_I}}$$

SUPPORTING INFORMATION AVAILABLE

Progress curves for the hydrolysis of substrate at various concentrations by the wild type and cc-mutant of *Dm*AChE in the absence and presence of paraoxon, where the difference between the theoretical curves when calculated by the explicit equation (Appendix) or by a numerically integrated system of differential equations is shown. This material is available free of charge via the Internet at http://pubs.acs.org.

REFERENCES

1. Rosenberry, T. L. (1975) Acetylcholinesterase. *Adv. Enzymol. 43*, 103–208.
2. Sussman, J. L., Harel, M., Frolow, F., Oefner, C., Goldman, A., Toker, L., and Silman, I. (1991) Atomic structure of acetylcholinesterase from *Torpedo californica*: A prototypic acetylcholine-binding protein. *Science 253*, 872–879.
3. Mallender, W. D., Szegletes, T., and Rosenberry, T. L. (2000) Acetylthiocholine binds to Asp74 at the peripheral site of human acetylcholinesterase as the first step in the catalytic pathway. *Biochemistry 39*, 7753–7763.
4. Stojan, J., Brochier, L., Alies, C., Colletier, J. P., and Fournier, D. (2004) Inhibition of *Drosophila melanogaster* acetylcholinesterase by high concentrations of substrate. *Eur. J. Biochem. 271*, 1364–1371.
5. Colletier, J. P., Fournier, D., Greenblatt, H. M., Stojan, J., Sussman, J. L., Zaccai, G., Silman, I., and Weik, M. (2006) Inhibition of *Drosophila melanogaster* acetylcholinesterase by high concentrations of substrate. *EMBO J. 25*, 2746–2756.
6. Gilson, M. K., Straatsma, T. P., McCammon, J. A., Ripoll, D. R., Faerman, C. H., Axelsen, P. H., Silman, I., and Sussman, J. L. (1994) Open "Back Door" in a Molecular Dynamics Simulation of Acethylcholinesterase. *Science 263*, 1276–1278.
7. Kovach, I. M., Qian, N., and Bencsura, A. (1994) Efficient product clearance through exit channels in substrate hydrolysis by acetylcholinesterase. *FEBS Lett. 349*, 60–64.
8. Greenblatt, H. M., Guillou, C., Guénard, D., Argaman, A., Botti, S., Badet, B., Thal, C., Silman, I., and Sussman, J. L. (2004) The Complex of a Bivalent Derivative of Galanthamine with *Torpedo* Acetylcholinesterase Displays Drastic Deformation of the Active-Site Gorge: Implications for Structure-Based Drug Design. *J. Am. Chem. Soc. 126*, 15405–15411.
9. Eastman, J., Wilson, E. J., Cervenansky, C., and Rosenberry, T. L. (1995) Fasciculin 2 binds to the peripheral site on acetylcholinesterase and inhibits substrate hydrolysis by slowing a step involving proton transfer during enzyme acylation. *J. Biol. Chem. 270*, 19694–19701.
10. Goliěnik, M., and Stojan, J. (2002) Multi-step analysis as a tool for kinetic parameter estimation and mechanism discrimination in the reaction between tight-binding fasciculin 2 and electric eel acetylcholinesterase. *Biochim. Biophys. Acta 1597*, 164–172.
11. Marchot, P., Khelif, A., Ji, Y. H., Mansuelle, P., and Bougis, P. E. (1993) Binding of ^{125}I-fasciculin to rat brain acetylcholinesterase. The complex still binds diisopropyl fluorophosphate. *J. Biol. Chem. 268*, 12458–12467.
12. Radić, Z., Duran, R., Vellom, D. C., Li, Y., Cervenansky, C., and Taylor, P. (1994) Site of fasciculin interaction with acetylcholinesterase. *J. Biol. Chem. 269*, 11233–12339.
13. Radić, Z., Quinn, D. M., Vellom, D. C., Camp, S., and Taylor, P. (1995) Allosteric control of acetylcholinesterase catalysis by fasciculin. *J. Biol. Chem. 270*, 20391–20399.
14. Bui, J. M., Tai, K., and McCammon, J. A. (2004) Acetylcholinesterase: Enhanced fluctuations and alternative routes to the active site in the complex with fasciculin-2. *J. Am. Chem. Soc. 126*, 7198–7205.
15. Tai, K., Shen, T., Borjesson, U., Philippopoulos, M., and McCammon, J. A. (2001) Analysis of a 10-ns molecular dynamics simulation of mouse acetylcholinesterase. *Biophys. J. 81*, 715–724.
16. Enyedy, I. J., Kovach, I. M., and Bencsura, A. (2001) Molecular dynamics study of active-site interactions with tetracoordinate transients in acetylcholinesterase and its mutants. *Biochem. J. 353*, 645–653.
17. Zhou, H. X., Wlodek, S. T., and McCammon, J. A. (1998) Conformation gating as a mechanism for enzyme specificity. *Proc. Natl. Acad. Sci. U.S.A. 95*, 9280–9283.
18. Szegletes, T., Mallender, W. D., and Rosenberry, T. L. (1998) Substrate binding to the peripheral site of acetylcholinesterase initiates enzymatic catalysis. Substrate inhibition arises as a secondary effect. *Biochemistry 37*, 4206–4216.
19. Nicolas, A., Ferron, F., Toker, L., Sussman, J. L., and Silman, I. (2001) Histochemical method for characterization of enzyme crystals: Application to crystals of *Torpedo californica* acetylcholinesterase. *Acta Crystallogr. D57*, 1348–1350.
20. Faerman, C., Ripoll, D., Bon, S., Le Feuvre, Y., Morel, N., Massoulie, J., Sussman, J. L., and Silman, I. (1996) Site-directed mutants designed to test back-door hypotheses of acetylcholinesterase function. *FEBS Lett. 386*, 65–71.
21. Kronman, C., Ordentlich, A., Barak, D., Velan, B., and Shafferman, A. (1994) The "back door" hypothesis for product clearance in acetylcholinesterase challenged by site-directed mutagenesis. *J. Biol. Chem. 269*, 27819–27822.
22. Velan, B., Barak, D., Ariel, N., Leitner, M., Bino, T., Ordentlich, A., and Shafferman, A. (1996) Structural modifications of the omega loop in human acetylcholinesterase. *FEBS Lett. 395*, 22–28.
23. Siadat, O. R., Lougarre, A., Lamouroux, L., Ladurantie, C., and Fournier, D. (2006) The effect of engineered disulfide bonds on the stability of *Drosophila melanogaster* acetylcholinesterase. *BMC Biochem. 7*, 12.
24. Chaabihi, H., Fournier, D., Fedon, Y., Bossy, J. P., Ravallec, M., Devauchelle, G., and Cerutti, M. (1994) Biochemical characterization of *Drosophila melanogaster* acetylcholinesterase expressed by recombinant baculoviruses. *Biochem. Biophys. Res. Commun. 203*, 734–742.
25. Kunkel, T. A. (1985) Rapid and efficient site-specific mutagenesis without phenotypic selection. *Proc. Natl. Acad. Sci. U.S.A. 82*, 488–492.
26. Estrada-Mondaca, S., and Fournier, D. (1998) Stabilization of recombinant *Drosophila* acetylcholinesterase. *Protein Expression Purif. 12*, 166–172.
27. Charpentier, A., Menozzi, P., Marcel, V., Villatte, F., and Fournier, D. (2000) A method to estimate acetylcholinesterase-active sites and turnover in insects. *Anal. Biochem. 285*, 76–81.
28. Ellman, G. L., Courtney, K. D., Andres, V., Jr., and Feather-Stone, R. M. (1961) A new and rapid colorimetric determination of acetylcholinesterase activity. *Biochem. Pharmacol. 7*, 88–95.
29. Fekonja, O., Zorec-Karlovsek, M., El Kharbili, M., Fournier, D., and Stojan, J. (2007) Inhibition and protection of cholinesterases by methanol and ethanol. *J. Enzyme Inhib. Med. Chem. 22*, 407–415.
30. Hames, B. (1981) An introduction to polyacrylamide gel electrophoresis, in *Gel electrophoresis of proteins, a practical approach* (Hames, B., and Richwood, D., Eds.) pp 1−91, IRS Press, Arlington, VA.
31. Karnovski, M., and Roots, L. (1964) A "direct-coloring" thiocholine method for cholinesterases. *J. Histochem. Cytochem. 12*, 219–222.
32. Fournier, D., Cuany, A., Bride, J. M., and Berge, J. B. (1987) Molecular polymorphism of head acetylcholinesterase from adult houseflies (*Musca domestica* L.). *J. Neurochem. 49*, 1455–1461.
33. Stojan, J., Goliěnik, M., and Fournier, D. (2004) Rational polynomial equation as an unbiased approach for the kinetic studies of *Drosophila melanogaster* acetylcholinesterase reaction mechanism. *Biochim. Biophys. Acta 1703*, 53–61.

34. Anfinsen, C. B., and Scheraga, H. A. (1975) Experimental and theoretical aspects of protein folding. *Adv. Protein Chem. 29*, 205–300.
35. Kauzmann, W. (1959) Some factors in the interpretation of protein denaturation. *Adv. Protein Chem. 14*, 1–63.
36. Matthews, B. W. (1995) Studies on protein stability with T4 lysozyme. *Adv. Protein Chem. 46*, 249–278.
37. Eriksson, A. E., Baase, W. A., Zhang, X. J., Heinz, D. W., Blaber, M., Baldwin, E. P., and Matthews, B. W. (1992) Response of a protein structure to cavity-creating mutations and its relation to the hydrophobic effect. *Science 255*, 178–183.
38. Pakula, A. A., and Sauer, R. T. (1990) Reverse hydrophobic effects relieved by amino-acid substitutions at a protein surface. *Nature 344*, 363–364.
39. Auerbach, G., Ostendorp, R., Prade, L., Korndorfer, I., Dams, T., Huber, R., and Jaenicke, R. (1998) Lactate dehydrogenase from the hyperthermophilic bacterium thermotoga maritima: The crystal structure at 2.1 Å resolution reveals strategies for intrinsic protein stabilization. *Structure 6*, 769–781.
40. Plaza del Pino, I. M., Ibarra-Molero, B., and Sanchez-Ruiz, J. M. (2000) Lower kinetic limit to protein thermal stability: A proposal regarding protein stability in vivo and its relation with misfolding diseases. *Proteins 40*, 58–70.
41. Clarke, J., and Fersht, A. R. (1993) Engineered disulfide bonds as probes of the folding pathway of barnase: Increasing the stability of proteins against the rate of denaturation. *Biochemistry 32*, 4322–4329.
42. Radić, Z., and Taylor, P. (1999) The influence of peripheral site ligands on the reaction of symmetric and chiral organophosphates with wild type and mutant acetylcholinesterases. *Chem.-Biol. Interact. 119−120*, 111–117.
43. Marcel, V., Estrada-Mondaca, S., Magne, F., Stojan, J., Klaebe, A., and Fournier, D. (2000) Exploration of the *Drosophila* acetylcholinesterase substrate activation site using a reversible inhibitor (Triton X-100) and mutated enzymes. *J. Biol. Chem. 275*, 11603–11609.
44. Goliěnik, M., Fournier, D., and Stojan, J. (2002) Acceleration of *Drosophila melanogaster* acetylcholinesterase methanesulfonylation: Peripheral ligand D-tubocurarine enhances the affinity for small methanesulfonylfluoride. *Chem.-Biol. Interact. 139*, 145–157.
45. Boublik, Y., Saint-Aguet, P., Lougarre, A., Arnaud, M., Villatte, F., Estrada-Mondaca, S., and Fournier, D. (2002) Acetylcholinesterase engineering for detection of insecticide residues. *Protein Eng. 15*, 43–50.
46. Brochier, L., Pontie, Y., Willson, M., Estrada-Mondaca, S., Czaplicki, J., Klaebe, A., and Fournier, D. (2001) Involvement of deacylation in activation of substrate hydrolysis by *Drosophila* acetylcholinesterase. *J. Biol. Chem. 276*, 18296–18302.
47. Marty, J. L., Sode, K., and Karube, I. (1992) Biosensor for detection of organophosphate and carbamate insecticides. *Electroanalysis,* 4.

BI7025479